

Measurement of Bunch Length Using Spectral Analysis of Incoherent Radiation Fluctuations*

V. Sajaev

Argonne National Laboratory, Argonne, Illinois 60439

Abstract. A measurement of the longitudinal beam profile of a relativistic charged particle beam is an important tool in modern accelerators. For bunch lengths in the range of picoseconds, such measurements can be performed by means of a streak camera. Shorter bunches usually require special techniques. In this paper we describe a novel technique that allows obtaining properties of a bunch of charged particles through measurement of the fluctuations of incoherent radiation from the bunch. Due to shot-noise fluctuations in the longitudinal beam density, this incoherent radiation has a spectrum, which consists of random spikes with width inversely proportional to the bunch length. The convolution of the beam current can also be obtained from the radiation spectrum. After the convolution function is found, the phase retrieval technique can be applied to recover the bunch shape. This technique has been used to analyze the shape of the 4-ps-long bunches at the Advanced Photon Source self-amplified spontaneous emission free-electron laser (SASE FEL) experiment.

INTRODUCTION

Recent developments in physics and technology open an exciting world of very short subpicosecond bunches. The length of electron bunches that are going to be used in the next linear colliders is of the order of 1 picosecond [1]. The projects of X-ray free-electron lasers (FELs) require even shorter bunches, down to 100 femtoseconds or less. The Linac Coherent Light Source (LCLS) [2] under construction at SLAC utilizes electron bunches as short as 80 femtoseconds to produce self-amplified spontaneous emission (SASE) radiation in an FEL. The new Subpicosecond Pulse Particle Source (SPPS) [3] already can produce electron pulses as short as 30 femtoseconds rms.

The production and tuning of these short bunches is crucial to the performance of these colliders and FELs, but the measurement of such ultrashort bunches is an interesting challenge itself. For bunch lengths in the range of picoseconds, such measurements can be performed with a streak camera. But shorter bunches require special techniques. They include high-power rf transverse deflecting structures that streak the beam in the accelerator allowing the bunch length to be observed on a profile monitor [4,5]. Electro-optic crystal diagnostics use the electric field of the electron bunch to modulate the light emitted by high-bandwidth, femtosecond visible lasers thereby allowing one to recover the bunch length [6]. Coherent synchrotron

* Work supported by U.S. Department of Energy, Office of Basic Sciences, under Contract No. W-31-109-ENG-38.

radiation from dipole magnets can also be detected in a terahertz band at wavelengths comparable to the bunch length [7].

In this paper we describe a method proposed previously [8, 9, 10], which allows obtaining properties of a bunch of charged particles through measurement of the fluctuations of incoherent emission from the bunch. Emission can be produced by any kind of incoherent radiation: generated in a bend or wiggler, transition or Cerenkov radiation, etc. And, unlike the techniques using coherent radiation, this method does not set any conditions on the bandwidth of the radiation. These conditions are rather set by available detectors.

This paper begins with a theoretical description of the method. Then it describes the instrumentation used for this experiment. The rest of the paper is devoted to the experimental results on single-shot spectral measurements and on recovery of the bunch profile. Simulation results are also presented to check and confirm the technique used.

THEORY

Let us consider a microscopic picture of the bunch, where each particle radiates an electromagnetic pulse with the electric field given by a function $e(t)$. (The specific expression for this function depends on how the radiation was generated: in the dipole, or in the wiggler, etc.) The total radiated field $E(t)$ of all particles is

$$E(t) = \sum_{k=1}^N e(t - t_k),$$

where N is the total number of particles in the bunch and t_k defines the longitudinal position of k -th particle within the bunch. We assume that t_k are random numbers, with the probability to find t_k between t and $t+dt$ equal to $f(t)dt$, where $f(t)$ is the bunch distribution function normalized to 1.

The spectral properties of the radiation can be obtained from the Fourier transform of the radiated field:

$$\hat{E}(\omega) = \int_{-\infty}^{\infty} E(t) e^{i\omega t} dt = \int_{-\infty}^{\infty} e^{i\omega t} dt \sum_{k=1}^N e(t - t_k) = \hat{e}(\omega) \sum_{k=1}^N e^{i\omega t_k},$$

where $\hat{e}(\omega) = \int_{-\infty}^{\infty} e(t) e^{i\omega t} dt$. In the real experiment, one measures the power spectrum

of the radiation $P(\omega)$, which is proportional to $|\hat{E}(\omega)|^2$ (for simplicity we take

$$P(\omega) = |\hat{E}(\omega)|^2):$$

$$P(\omega) = \hat{E}(\omega) \cdot \hat{E}^*(\omega) = \hat{e}(\omega) \hat{e}^*(\omega) \sum_{k=1}^N e^{i\omega t_k} \sum_{m=1}^N e^{-i\omega t_m} = |\hat{e}(\omega)|^2 \sum_{k,m=1}^N e^{i\omega(t_k - t_m)}. \quad (1)$$

Averaging this equation, we find

$$\langle P(\omega) \rangle = |\hat{e}(\omega)|^2 \sum_{k,m=1}^N \int_{-\infty}^{\infty} \int_{-\infty}^{\infty} dt_k dt_m f(t_k) f(t_m) e^{i\omega(t_k - t_m)}$$

$$\begin{aligned}
&= |\hat{e}(\omega)|^2 \sum_{k=m}^N \int_{-\infty}^{\infty} \int_{-\infty}^{\infty} dt_k dt_m f(t_k) f(t_m) e^{i\omega(t_k - t_m)} + |\hat{e}(\omega)|^2 \sum_{k \neq m}^N \int_{-\infty}^{\infty} \int_{-\infty}^{\infty} f(t_k) e^{i\omega t_k} dt_k f(t_m) e^{-i\omega t_m} dt_m \\
&= |\hat{e}(\omega)|^2 (N + N^2 |\hat{f}(\omega)|^2), \tag{2}
\end{aligned}$$

where $|\hat{f}(\omega)|$ is the Fourier transform of the distribution function, and we used the approximation $N-1 \approx N$. The first term in Equation (2) is incoherent radiation proportional to the number of particles in the bunch. The second term is the coherent radiation that scales quadratically with N . The coherent radiation term carries information about the distribution function of the beam but only at low frequencies of the order of $\omega \cong \sigma_t^{-1}$, where $\hat{f}(\omega)$ is not zero. At high frequencies $N |\hat{f}(\omega)|^2 \ll 1$, and the coherent radiation is negligible in comparison with the incoherent one.

To illustrate the difference between coherent and incoherent radiation intensities, let us consider a numerical example for the case of a Gaussian beam with $\sigma_t = 1$ ps and total charge of 1 nC (approximately 10^{10} electrons). The Gaussian distribution function and its Fourier transform have the form:

$$f(t) = \frac{1}{\sqrt{2\pi}\sigma_t} e^{-\frac{t^2}{2\sigma_t^2}} \quad \text{and} \quad \hat{f}(\omega) = e^{-\frac{\omega^2 \sigma_t^2}{2}}. \tag{3}$$

At 1 THz frequency, where $\omega\sigma_t \approx 1$, the coherent term in Equation (2) is about 10^{10} times stronger. At $\omega\sigma_t = 10$, the coherent term is 10^{34} times weaker.

However, the original, not averaged expression for the spectral power (Equation (1)) shows that the properties of the radiation, even at high frequencies, carry information about the distribution function. Considered separately, each term of the summation $e^{i\omega(t_k - t_m)}$ oscillates as a function of frequency with the period $\Delta\omega = 2\pi/(t_k - t_m) \sim 2\pi/\sigma_t$. Because of the random distribution of particles in the bunch, the sum in Equation (1) fluctuates randomly as a function of frequency ω , and statistical properties of these fluctuations depend on the properties of the distribution function of the bunch.

To obtain quantitative characteristics of the radiation, let us calculate the average value of the product $P(\omega)P(\omega')$, which later can be used for calculation of the power spectrum autocorrelation:

$$\langle P(\omega)P(\omega') \rangle = |\hat{e}(\omega)|^2 |\hat{e}(\omega')|^2 \left\langle \sum_{k,m,p,q=1}^N e^{i\omega(t_k - t_m) + i\omega'(t_p - t_q)} \right\rangle.$$

The N^4 terms in this summation can be placed in 15 different classes (see Ref. 11). For the incoherent radiation, only two classes are important: $k=m, p=q, k \neq p$ and $k=q, m=p, k \neq m$. Thus it can be found that

$$\langle P(\omega)P(\omega') \rangle = N^2 |\hat{e}(\omega)|^2 |\hat{e}(\omega')|^2 \left(1 + |\hat{f}(\omega - \omega')|^2 \right). \tag{4}$$

We can now define the following second-order correlation function:

$$g(\omega - \omega') = \frac{\langle P(\omega)P(\omega') \rangle}{2 \langle P(\omega) \rangle \langle P(\omega') \rangle},$$

and, using Equations (2) and (4), it follows that

$$g(\Omega) = \frac{1}{2} \left(1 + |\hat{f}(\Omega)|^2 \right). \quad (5)$$

This important equation relates the spectrum autocorrelation function and the Fourier transform of the bunch shape. It can be used to find the bunch length.

Another useful quantity was introduced previously [9]. It is the Fourier transform of the spectrum

$$G(\tau) = \int_{-\infty}^{\infty} P(\omega) e^{i\omega\tau} d\omega.$$

It can be shown, that the variance, $D(\tau) = \left\langle |G(\tau) - \langle G(\tau) \rangle|^2 \right\rangle$, is proportional to the convolution function of the distribution function $f(t)$

$$D(\tau) = A \int_{-\infty}^{\infty} f(t) f(t-\tau) dt. \quad (6)$$

Strictly speaking, knowledge of the spectral function $|\hat{f}(\omega)|$ (or convolution function) does not allow a unique restoration of $f(t)$, because the information about the phase of $|\hat{f}(\omega)|$ is lost. However, as has been shown [12], using a phase-retrieval technique, one can recover the beam profile in many practical cases. This technique will be discussed later.

The above consideration assumes a filament beam, with a negligibly small transverse size. In this case, the fluctuations of the spectral intensity $P(\omega)$ are 100%, and the correlation function g in Equation (5) varies from 1 at $\Omega=0$ to 1/2 at $\Omega \rightarrow \infty$. This regime requires that the transverse beam size be smaller than the transverse coherence size of the radiation, which is of the order of $\lambda/2\pi\sigma_\theta$, where σ_θ is the angular spread of the radiation. In the opposite case, the fluctuations become less pronounced.

We also used a classical description of the radiation process and neglected quantum effects. This approach is justified if the quantum fluctuations of the number of radiated photons are negligible. One can derive the condition for the beam intensity when this requirement is met. If the source of the radiation is synchrotron light from a dipole, the number of photons that reach the detector in the frequency interval $\Delta\omega$ (they are radiated from $(1/\gamma)(\omega_c/\omega)^{1/3}$ radians of the beam trajectory, where ω_c is the critical frequency of the synchrotron radiation) can be estimated as [13]

$$\langle n_{ph} \rangle \approx \frac{1}{2} \alpha N_e \frac{\Delta\omega}{\omega},$$

where α is the fine structure constant, and N_e is the number of particles in the bunch. Assuming $\Delta\omega \sim \sigma_r^{-1}$ and visible light range, we can rewrite this equation as $\langle n_{ph} \rangle \approx 3 \cdot 10^5 (I / I_A)$, where I is the peak current in the beam and $I_A=17$ kA is the Alfven current. If the number of photons is much larger than one, the quantum effects can be neglected.

For wiggler radiation, the estimate for the number of radiated photons is

$$\langle n_{ph} \rangle \approx 4\alpha N_e M \frac{K^2}{1+K^2} \frac{\Delta\omega}{\omega},$$

where K is the wiggler parameter and M is the number of periods in the wiggler.

If condition $\langle n_{ph} \rangle \gg 1$ is not met, quantum fluctuations superimpose on the random fluctuations described above. However, the information about the pulse shape is still present in the measured signal. Although a larger statistics would be required to suppress the additional noise introduced by quantum fluctuations.

Finally, we would like to emphasize that measurements of the beam profile using spectral fluctuations can be done in one shot, if the width of the measured spectrum is wide enough. In this case, the averaging of different quantities can be done over the spectrum, rather than over multiple shots.

MEASUREMENTS

Recently, a number of measurements were reported that confirm the fluctuational nature of the spontaneous incoherent radiation. Most of these measurements were conducted at FEL-related facilities. First measurements of the single-shot spectra of the undulator spontaneous emission with resolution sufficient to demonstrate 100% fluctuations of intensity were performed at ATF/BNL [14]. Bunch length was extracted from the fluctuations, and emittance was estimated in that experiment. More extensive analysis of the spectral fluctuations was conducted at the Low-Energy Undulator Test Line (LEUTL) at the Advanced Photon Source at ANL [15]. Later, there were a number of reports demonstrating spectral fluctuations of synchrotron [16], Cerenkov [17], and transition radiation [18].

LEUTL Facility Description

In this part, we will describe in detail the results of single-shot spectrum measurements obtained at LEUTL.

The LEUTL system was built as an extension of the existing APS linac (Figure 1). It consists of a high-brightness photocathode rf electron gun coupled to the 650 MeV APS linac and a long undulator system. The gun is driven by a picosecond Nd:glass laser and can generate a few-picosecond electron pulses at 6 Hz frequency. A bunch compressor is installed after two accelerating sections of the linac to further reduce the electron bunch length. It is capable of compressing the beam by a factor of ten. The undulator system consists of nine identical 2.4-m-long sections separated by drift spaces where visible light diagnostics (VLD) stations are installed. Each VLD can deflect the undulator light and send it to the end station located at the downstream end of the undulator line.

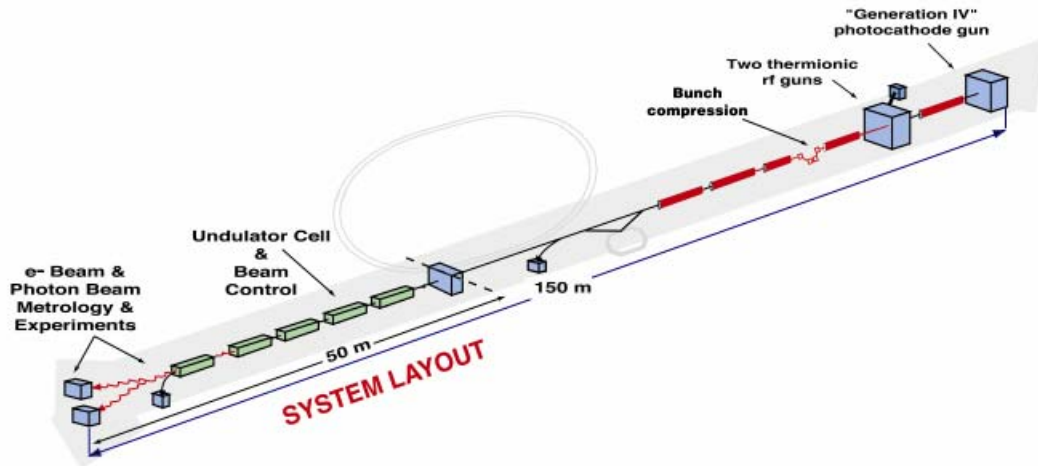


Figure 1. Schematic of the LEUTL system.

All spectral measurements reported in this paper have been obtained with a high-resolution spectrometer located at the downstream end of the undulator line in the end station. A mirror at each diagnostic station could direct the SASE light towards the spectrometer through a hole in the shielding wall, thus allowing one to measure spectral characteristics of the SASE light at different longitudinal locations along the undulator line.

A schematic of the spectrometer is shown in Figure 2. It utilizes a Paschen-Runge mount. This design was chosen because of its great flexibility: it provides independence on the angle of the incoming light, it can be tuned for wide range of wavelengths, and it is easy to modify. The spectrometer consists of three main elements all located on the Rowland circle: a vertical entrance slit, a spherical grating, and a CCD camera. The light coming from the undulator hall is focused on the entrance slit with a concave mirror. All optical elements are reflective with metal coatings. This allows the system to work over a wide range of wavelengths. The gated CCD camera can measure the radiation of each electron bunch separately. To reduce the dark current and to improve the signal-to-noise ratio, the CCD camera is cooled.

The spectrometer was calibrated with hollow cathode discharge lamps, and the designed resolution was checked on different wavelengths. The main parameters of the spectrometer are presented in Table 1.

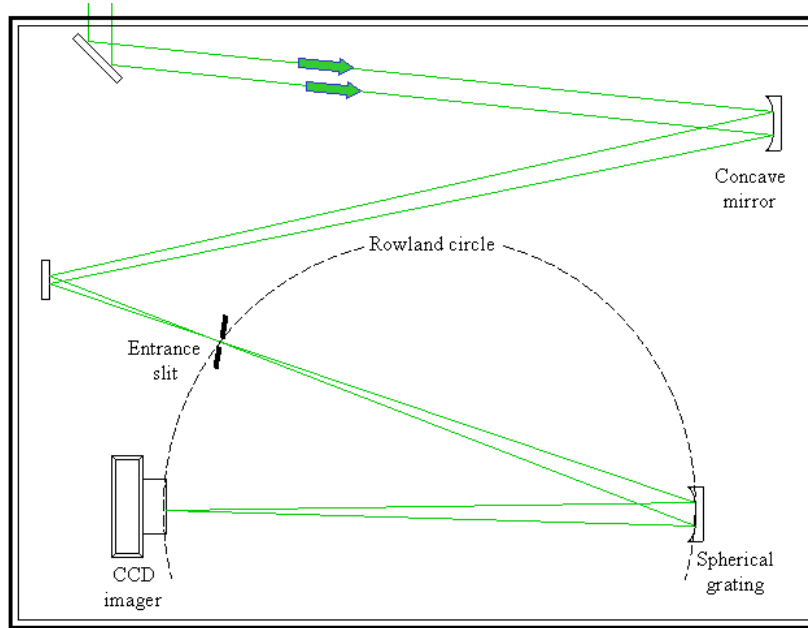


Figure 2. A top view of the Paschen-Runge-type spectrometer for the analysis of the SASE FEL light.

Table 1. Main parameters of the high-resolution spectrometer

Grating	Grooves/mm	600
	Curvature radius [mm]	1000
	Blaze wavelength [nm]	482
CCD camera	Number of pixels	1100×330
	Pixel size [μm]	24
Concave mirror curvature radius [mm]		4000
Spectral resolution [\AA]		0.4
Bandpass [nm]		44
Resolving power at 530 nm		10000
Wavelength range [nm]		250 – 1100

Spectrum measurements and bunch length extraction

Measurement of the typical single-shot spectrum is shown in Figure 3 (top). The spectrum is composed of spikes of random amplitude and frequency that have a characteristic width $\Delta\omega \sim 1/\sigma_t$ and intensity fluctuation of almost 100%. The shape of the individual spectra changes randomly from shot to shot, but the average of many shots approaches the familiar wiggler spectrum, Figure 3 (bottom).

To illustrate the spike width dependence on the bunch length, the bunch was compressed by the bunch compressor. Figure 4 presents the spectrum radiated by this much shorter bunch.

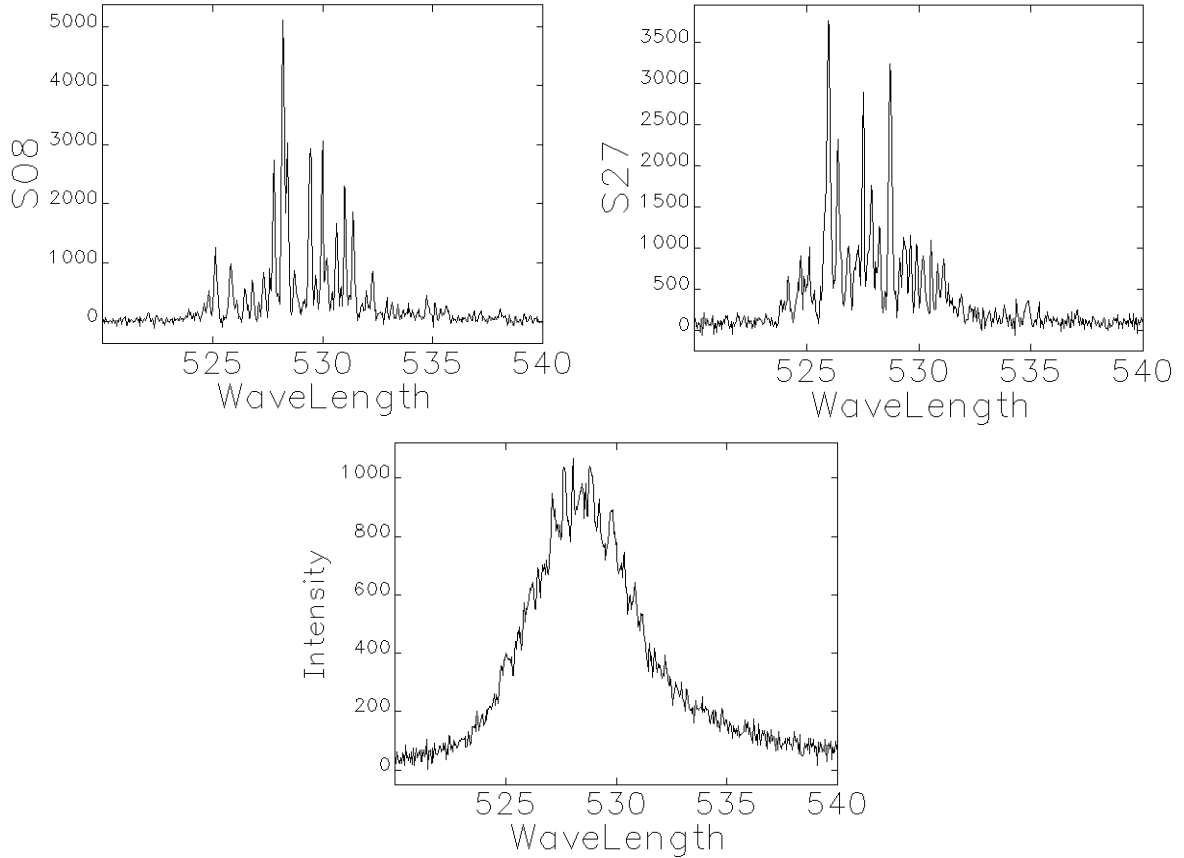


Figure 3. Top – examples of typical single-shot spectrum, bottom – spectrum averaged over 100 single shots.

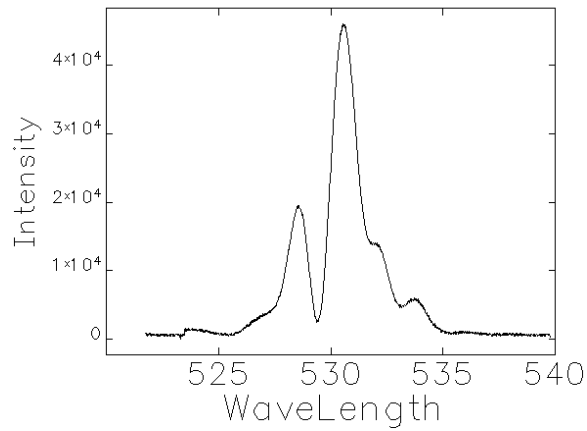


Figure 4. Single-shot spectrum for a very short bunch. The bunch was compressed by about a factor of 5 compared to the previous figure.

To extract the bunch length from the spectral data, Equation (5) for the second-order spectrum correlation is used. The normalized correlation of the spectral intensity averaged over many shots was calculated from the spectrum measurements:

$$C_n = \left\langle \sum_i P(\omega_i) P(\omega_{i+n}) \right\rangle / \left\langle \sum_i P(\omega_i)^2 \right\rangle,$$

where $P(\omega_i)$ is the signal in the i -th CCD channel and n is the shift in channels. The correlation averaged over 100 shots is plotted in Figure 5. To illustrate how the instrument resolution can affect the measurements, different sizes of the entrance slit of the spectrometer were used.

For the ideal case of a zero-emittance beam and a diagnostics with sufficient spectral resolution, 100% fluctuation of the spectral intensity will occur. However, when the beam size is large or the detector spectral resolution is poor, the spectrum will be similar to a spectrum emitted by several independent sources. The fluctuation level will be reduced, and a nonzero pedestal will appear in the spectrum.

In general, to achieve the best resolution, the entrance slit of the spectrometer should be less than the pixel size of the detector. But in our case the radiation intensity was not enough to work with slit openings less than 25 μm . Low resolution can lead to a situation where one detector channel sees more than one spike, which hampers the spike width measurements. The asymptotic level of the correlation curves at large n shows how large the pedestal was; for 100% intensity fluctuations, this level should be equal to 0.5 (see Equation (5)). The value of this level can be used to characterize how many independent modes contributed to the radiation measured in one channel. To be able to directly apply Equation (5), the curve with the smallest pedestal should be chosen.

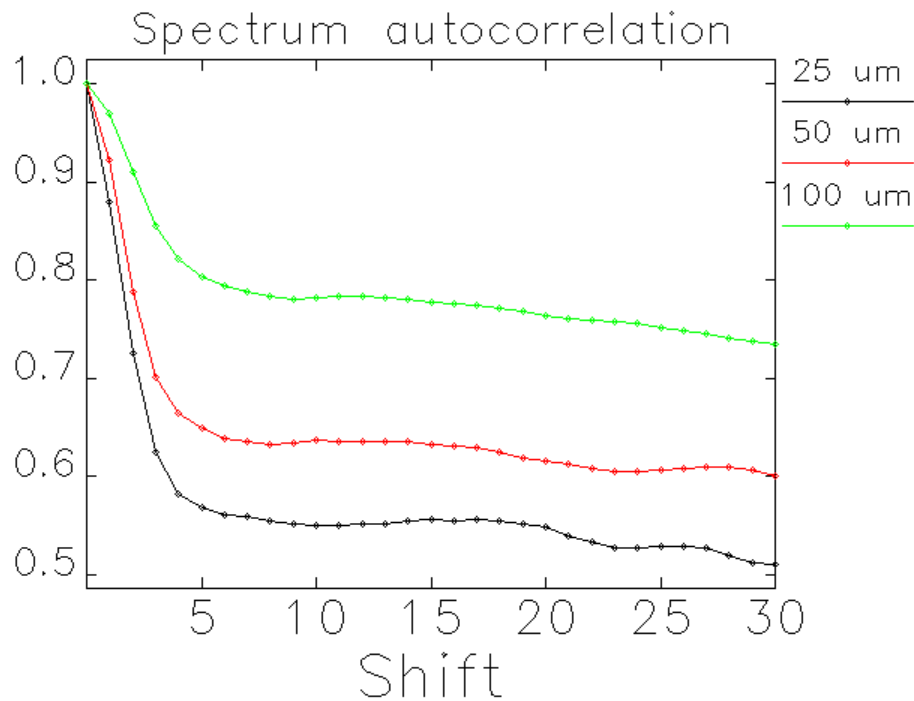


Figure 5. Spectrum autocorrelation for different entrance slit sizes. This plot illustrates how the instrument resolution can affect the measurements.

The spike width on half maximum according to Figure 5 is about two pixels. The frequency step corresponding to one pixel is $\delta\omega = 2.4 \cdot 10^{11}$ rad/s. Therefore, assuming the beam to be Gaussian and using Equations (3) and (5), the sigma of the Gaussian distribution is

$$\tau_b \approx \frac{1}{n \cdot \delta\omega} \approx 2 \text{ ps}.$$

This gives the FWHM length of the bunch to be equal to 4.5 ps.

The accuracy of determination of the spike width is not so great because its size is only a few pixels. This means the resolution of the spectrometer is not enough for these bunch lengths. But the shorter the bunch, the wider the spikes, and the higher the accuracy, see, for example, Figure 4.

Calculation of the convolution function of the bunch profile

As mentioned before, measurements of the spectral intensity fluctuations can be used not only to determine the bunch length but also to recover a longitudinal bunch profile. It has been shown [9] that the variance of the Fourier transform of the spectrum is proportional to the convolution function of the beam current. After the convolution function is found, a phase retrieval technique can be used to recover the shape of the pulse in many practical cases. These two steps are described below.

First, to calculate the convolution of the bunch current, we calculate the Fourier transform of the measured spectrum for measurement n :

$$G_{k,n} = \sum_{m=1}^{N_{ch}} P_{m,n} e^{2\pi i m k / N_{ch}},$$

where m and N_{ch} is the channel number and the number of channels in the detector (CCD), respectively, and P is the detector signal. After accumulation of N_p number of pulses large enough for statistical analysis, the variance of the Fourier transformed spectrum is calculated the following way:

$$D_k = \sum_{m=1}^{N_p} \left| G_{k,m} - \frac{1}{N_p} \sum_{n=1}^{N_p} G_{k,n} \right|^2.$$

It can be described in other words as the average deviation of the signal in the k -th channel from its average. As was mentioned above (see Equation (6)), the quantity D_k gives the convolution function of the particle density in the bunch averaged over N_p bunches.

Computer simulations have been performed to check this statement and confirmed it for bunches with Gaussian and step-function profiles. Figure 6 shows results of the simulation.

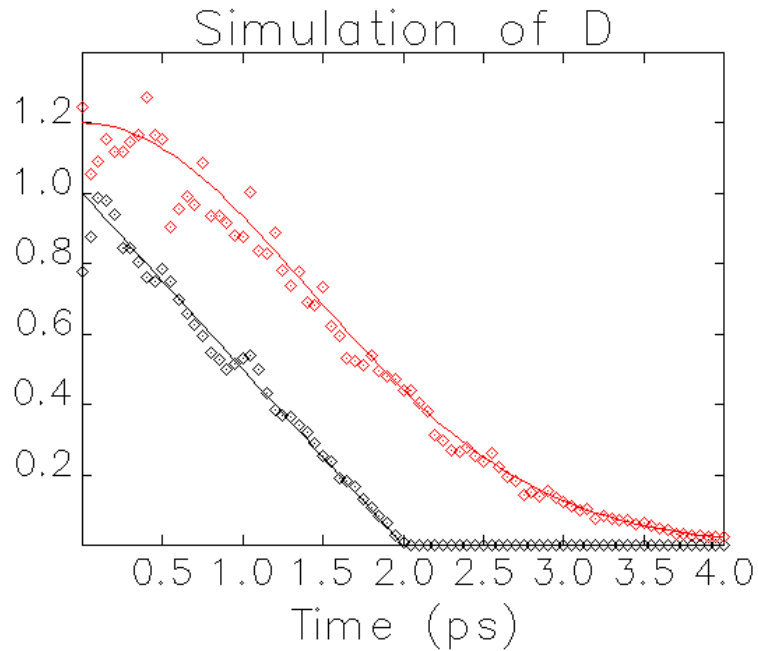


Figure 6. Convolutions of longitudinal bunch shape extracted from simulated single-shot spectra for Gaussian (red) and step-function (black) distributions. The number of particles used for the simulations was 100. The number of spectra for averaging was 200. Solid lines are analytical convolutions.

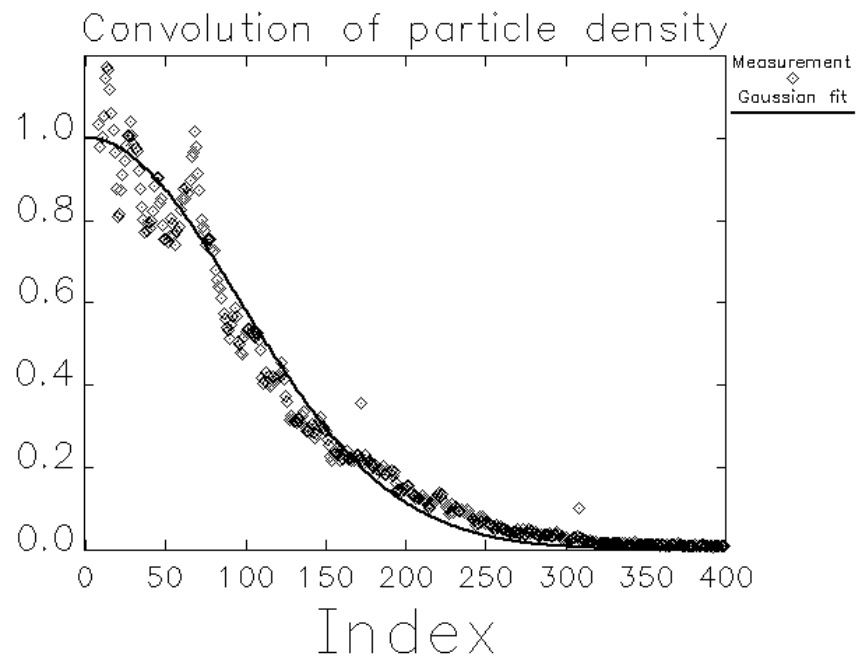


Figure 7. Convolution of longitudinal particle density calculated using measured spectra. Solid line is a fitted Gaussian function.

Figure 7 represents the convolution function of the longitudinal bunch distribution extracted from real spectral measurements. The number of spectrum measurements used for analysis is 100. This plot can also be used to determine the bunch length. If

we assume that the bunch has a Gaussian shape, then its convolution is also a Gaussian with $\sigma = \sqrt{2} \cdot \sigma_t$. A fitted Gaussian function is also shown in Figure 7 as a solid line. This plot gives the bunch length equal to $\tau_b = 1.8 ps$.

As mentioned above, the convolution function of the bunch profile does not allow for a strict restoration of the bunch profile itself. But, in practice, real beams often look like some nonsymmetric combination of flattop and ‘‘Gaussian-like’’ functions. For these cases, using the Gaussian function alone to fit the convolution gives a good enough answer for the bunch length.

Reconstruction of the bunch shape from the convolution function

If the measurement of the bunch length using the convolution techniques described above does not provide enough information, one can apply a more sophisticated analysis of the convolution function. It is possible to extract both the amplitude and the phase information of the radiation source by applying a Kramers-Kronig relation to the convolution function. This technique of phase extraction was well developed in the optics of solids for the problem of reflectivity. We will briefly describe the technique following Ref. [12].

We denote the longitudinal particle density as $S(z)$ and its Fourier transform as $S(\omega)$ and write it in the following form

$$S(\omega) = \rho(\omega)e^{i\psi(\omega)}. \quad (7)$$

Here $\rho(\omega)$ corresponds to the Fourier transform of our convolution function. Phase ψ can be extracted using the expression

$$\psi_m(\omega) + \psi_{Blaschke}(\omega) = -\frac{2\omega}{\pi} P \int_0^\infty dx \frac{\ln \rho(x)}{x^2 - \omega^2} + \sum \arg \left(\frac{\omega - \omega_j}{\omega - \omega_j^*} \right),$$

where ψ_m is the minimal phase and the ω_j 's are the zeros of $S(\omega)$ in the upper half of the complex frequency plane. If $S(\omega)$ has no zeros, the contribution from $\psi_{Blaschke}(\omega)$ equals zero, and the expression above gives the minimal phase. This minimal phase is a good approximation to the actual phase in cases where the bunch density has no nearby zeros in the upper half of the complex frequency plane. The final expression for calculating the minimal phase is

$$\psi_m(\omega) = -\frac{2\omega}{\pi} P \int_0^\infty dx \frac{\ln[\rho(x)/\rho(\omega)]}{x^2 - \omega^2}.$$

Introduction of $\rho(\omega)$ in the numerator of the integral does not change the principal value of the integral and removes the singularity at $x=\omega$. The density distribution function can now be obtained from the inverse Fourier transform of Equation (7):

$$S(z) = \frac{1}{\pi c} \int_0^\infty d\omega \cdot \rho(\omega) \cdot \cos \left(\psi_m(\omega) - \frac{\omega z}{c} \right).$$

Figure 8 shows the simulated results of applying the above technique to restore different bunch shapes. The solid line is the original bunch shape, and the dots are distribution functions calculated from the convolution function with minimal phase

approximation. One can see that, for some bunch shapes, this technique gives really good agreement, while for others it is not as good.

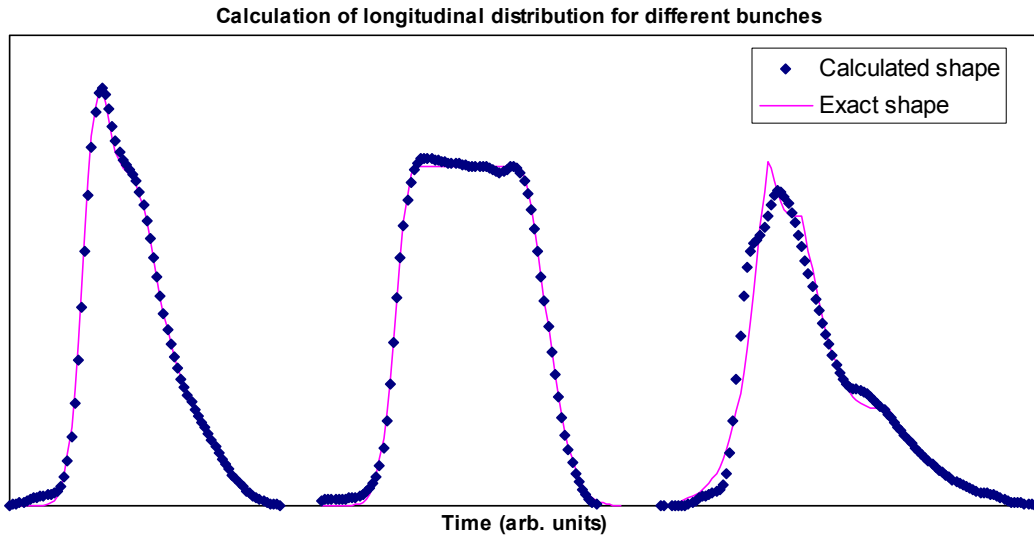


Figure 8. Simulation: exact longitudinal bunch distribution function compared with that calculated from the convolution function. First – sum of three Gaussian functions; second – step function combined with Gaussians; third – sum of three Gaussian-like functions $e^{-\frac{z^{1.3}}{2 \cdot \sigma^{1.3}}}$.

Next, the technique described above is applied to the measured convolution function of the longitudinal bunch distribution (Figure 7). One can see that the plot of the convolution function is still very noisy despite analyzing 100 single shots. This noise produces high-frequency content in the Fourier transformation. Therefore, before taking the Fourier transform of the convolution function, it has been smoothed by filtering out the high frequencies.

Results of calculations of the bunch shape for two different measurements (two sets of 100 single-shot spectra) are presented in Figure 9. They were taken on the same day with an interval of several hours. The electron beam parameters were supposed to be the same, but small variations were possible. The two curves demonstrate almost the same profile of the beam with a FWHM length of approximately 4 ps.

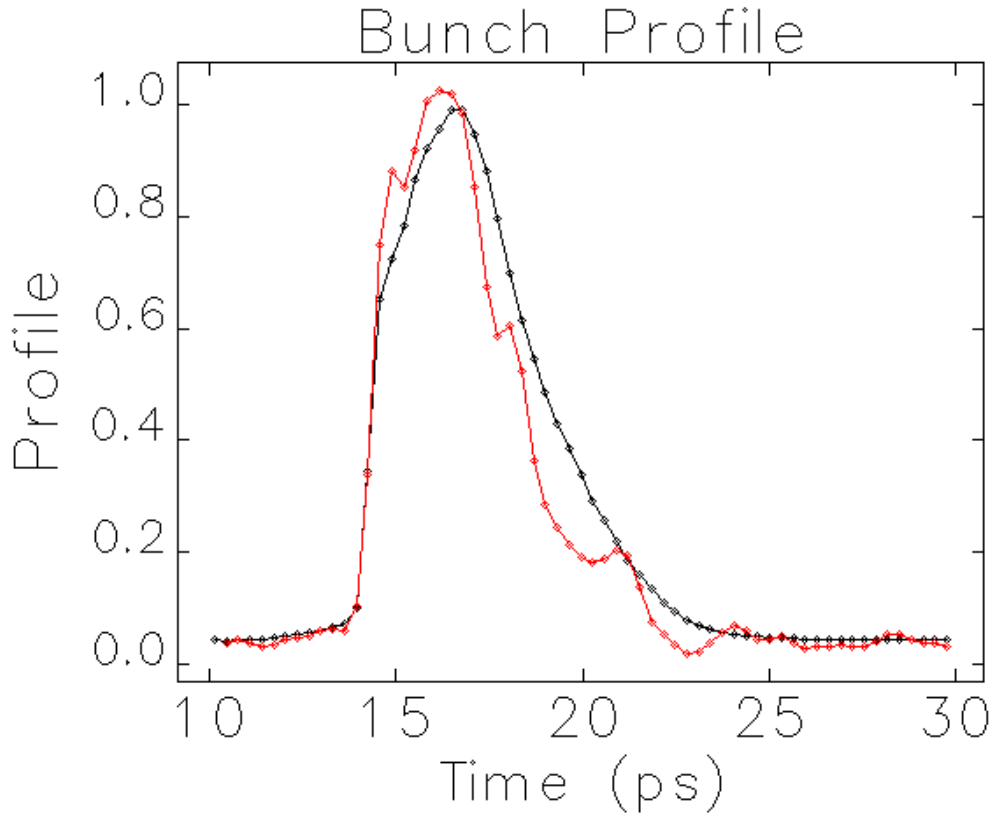


Figure 9. Bunch shape calculated from two different sets of measurements. The beam parameters were approximately the same, and the calculations show similar bunch profile for both measurements.

CONCLUSIONS

A technique for recovering a longitudinal bunch profile from spectral fluctuations of incoherent radiation has been implemented, and a bunch profile of a relatively short 4-ps beam has been measured. Although we used synchrotron radiation above, the nature of the radiation is not important, it can be transition radiation, Cerenkov, etc. Typically, averaging over many (of the order of 10^2) single shots is required, however a modification of the method is possible in which one can perform averaging over wide spectral intervals in a single pulse.

To reconstruct the bunch shape from the convolution function we used the technique suggested in Ref. [12], but we used a different approach to build the convolution. Using spectrum fluctuations to construct the convolution allows us to avoid measuring the spectrum of coherent far infrared radiation of the bunch and making any assumptions about the asymptotic behavior of this spectrum.

An important feature of the method is that it can be used for bunches with lengths varying from a centimeter to tens of microns. However, there are several important conditions for this technique. In order to be able to measure a bunch of length σ_b , the spectral resolution of the spectrometer should be better than $1/\sigma_b$. Also, the spectral width of the radiation and the spectrometer must be much larger than the inverse bunch length. For example, Figure 4 presents the situation when the radiation

bandwidth (wiggler radiation) is not large enough; therefore one can observe only a few spectral spikes.

ACKNOWLEDGMENTS

The author would like to thank Max Zolotarev and Gennady Stupakov for very useful discussions on the method, Steve Milton and Efim Gluskin for stimulating and supporting this work, and Oleg Makarov for discussions and help with the measurements.

REFERENCES

-
1. "Zeroth-Order Design Report for the Next Linear Collider," LBNL-PUB-5424, SLAC Report 474 (May 1996).
 2. "LCLS CDR", SLAC-R-593, April 2002.
 3. M. Cornacchia et al., "A Subpicosecond Photon Pulse Facility for SLAC," SLAC-PUB-8950, LCLS-TN-01-7, Aug. 2001.
 4. R.H. Miller, R.F. Koontz, D.D. Tsang, "The SLAC Injector," IEEE Trans. Nucl. Sci., June 1965, p 804.
 5. X.-J. Wang, "Producing and Measuring Small Electron Bunches," Proc. of the PAC 1999.
 6. X. Yan et al., Phys. Rev. Lett. 85, 3404 (2000); I. Wilke et al., Phys. Rev. Lett. 88, 124801 (2002).
 7. T. Nakazato, et al., Phys. Rev. Lett. 63, 1245 (1989); Y. Shibata, et. al., Nucl. Instrum. Methods Phys. Res. Sect. A 301, 161 (1991); E. B. Blum, U. Happek and A. Sievers, Nucl. Instrum. Methods Phys. Res. Sect. A 307, 568 (1991).
 8. M.S. Zolotarev, G.V. Stupakov, "Fluctuational Interferometry for Measurements of Short Pulses of Incoherent Radiation," SLAC Rep. SLAC-PUB-7132, 1996.
 9. M.S. Zolotarev, G.V. Stupakov, "Spectral Fluctuations of Incoherent Radiation and Measurement of Longitudinal Bunch Profile," Proc. of the 1997 Particle Accelerator Conference.
 10. J. Krzywinski, E. Saldin, E. Schneidmiller and M. Yurkov, "A New method for Ultrashort Electron Pulse-Shape Measurement Using Synchrotron Radiation from a Bending Magnet," DESY Report DESY-TESLA-FEL 97-03.
 11. J. Goodman, *Statistical Optics*, J. Willey and Sons, New York, 1985.
 12. R. Lai, A.J. Sievers, Micro Bunches Workshop, AIP Conference Proceedings 367 (NY), p. 312, 1995.
 13. M. Sands, SLAC Rep. SLAC-121, 1970.
 14. P. Catravas et al., Phys. Rev. Lett., **82**, 5261-5264 (1999).
 15. V. Sajaev, "Determination of Longitudinal Bunch Profile using Spectral Fluctuations of Incoherent Radiation," Proc. of EPAC 2000, p. 1806.
 16. L. DiMauro, et al., "First SASE and seeded FEL lasing of the NSLS DUV FEL at 266 and 400 nm"; A. Murokh, et al., "Results of the VISA SASE FEL Experiment at 840 nm"; V. Ayvazyan, et al., "Study of the Statistical Properties of the Radiation from a VUV SASE FEL Operating in the Femtosecond Regime." All in Proc. of FEL Conference 2002.
 17. T. Wanabe, et al., "Diagnostics of Subpicosecond Electron Pulse by the Fluctuation Method," Proc. of PAC 2001, p. 2362.
 18. A. Lumpkin, et al., "Evidence for Micro-Bunching in a Saturated Free-Electron Laser Using Coherent Optical Transition Radiation," Phys. Rev. Lett., 88, 234801 (2002).